Predictive Maneuver Planning for an Autonomous Vehicle in Public Highway Traffic

Qian Wang[iD], Beshah Ayalew[iD], *Member, IEEE*, and Thomas Weiskircher[iD]

Abstract—This paper outlines a predictive maneuver-planning method for autonomous vehicle navigating public highway traffic. The method integrates discrete maneuvering decisions, i.e., lane and reference speed selection automata, with a model predictive control-based motion trajectory-planning scheme. A key notion is to apply a predictive reference speed pre-planning for each lane at each time step of a selected prediction horizon. This is done based on the predicted likely motion of the autonomous vehicle and other object vehicles subject to sensor noise and environmental disturbances. Then, an optimization problem is configured that computes safe, sub-optimal plans for the trajectories of both the motion states (and inputs) and maneuver references for the prediction horizon to accomplish maneuvers like lane keeping, lane change, or obstacle avoidance. While a first formulation of the problem results in a mixed-integer nonlinear programming problem, it is shown that a relaxation can be adopted that reduces the computational complexity to a low-order polynomial time nonlinear program that can be solved more efficiently. Through simulation of a series of multi-lane highway scenarios and comparison with one-maneuver planning approach and an adaptive cruise control approach, the proposed predictive maneuver planning is illustrated to better accommodate the traffic environment with feasible execution time. Also, the reference speed pre-planning improves the optimality and the robustness of the maneuver decision in trajectory planning without adding computational complexity to the optimization problem.

Index Terms—Autonomous vehicle, predictive maneuver planning, predictive trajectory planning, hybrid system modeling.

I. INTRODUCTION

AUTONOMOUS driving is a promising technology for improving the safety, efficiency and environmental impact of on-road transportation systems. Despite the existence of elegant algorithms [1] for route or global path planning from position A to B, the task of guiding an autonomous vehicle to rapidly and systematically accommodate the plethora of changing constraints for local motion planning in public traffic is a challenge problem. These constraints arise from tire/road friction conditions, avoiding

stationary and moving obstacles, obeying the traffic rules, signals and so on. One of the core problems is designing robust and computationally efficient trajectory planning algorithms that can generate the appropriate vehicle maneuvers as well as the constituent motion trajectories while considering the differential vehicle dynamics of the controlled vehicle and the listed constraints in public traffic with measurement noise and other uncertainties. Plenty of methods have been proposed to deal with this problem, as also summarized in [2] and [3]. They roughly fall into three groups: sampling-based planning methods, path-velocity decomposition methods and numerical optimization methods.

Sampling-based planning methods are popular methods for trajectory guidance of robotic vehicles. The methods discretize/sample the state space of the motion into a library of quantized motion primitives/lattices [4], obtained from numerically solving the steady state or transient vehicle dynamic motion models. As each primitive/lattice indicates a maneuver, the methods are also called maneuver-based planning methods [5]. Then, efficient heuristics for deterministic or stochastic searching, such as the A* algorithm [6] or RRT* based algorithm [7], can be applied in real-time to construct a periodic planning law from the library, ensuring some robustness and safety in a disturbance environment. However, the completeness and optimality of these methods depend strongly on the resolution of the library. The complexity of finding the best trajectory increases with the resolution of the library. Also, the resulting non-continuous trajectory induces jerky, uncomfortable motions.

Path-velocity decomposition methods decompose the planning work into two sub-problems: local path planning and path-tracking. Graph-search based method like Dijkstra's Algorithm [8] and A* algorithm [9] or interpolating curves like clothoid curves [10], polynomial curves [11] and Bezier curves [12] are used in the local path planner design to generate the way points in the 2D configuration space. Then, a closed-loop controller is applied to track the path while satisfying the constraints in work space. However, as the planned path is not often given as a function of time, collision-free motion is not guaranteed by following the path. Therefore, the robustness and safety of the decomposition methods highly depend on the quality of the path-tracking controller.

On the other hand, the numerical optimization methods find the best trajectory by solving constrained optimization problems. These methods can naturally handle multiple constraints and uncertainties but they suffer from the

computational burden of optimizing the motion state over a future horizon from a current time step. Therefore, in practical applications, these methods usually follow a receding horizon pattern with a limited horizon length in a scheme also known as model predictive control (MPC). These use fast real-time solvers [13], [14] to periodically solve the optimization problems, where only a first section (step) of the input trajectory is executed and the process is repeated in receding prediction horizons. MPC, which initially was applied to modeling human-driver like control in various traffic situations [15], it now appears in many works as a reactive planner for autonomous and semi-autonomous vehicle control [16]–[19]. To apply MPC for trajectory planning requires the knowledge of global route waypoints as references to follow. For the on-road scenario, the centerline of each lane from the perception or map information [20], [21] can be used as the reference path. For off-road scenarios, this method can be incorporated in the path tracking level the path-velocity decomposition methods [22]. In addition, specific terminal costs and constraints could be designed to circumvent limitations of robustness and stability that arise from the use of finite horizons [23], [24].

In MPC-based trajectory planning, the expected states of the autonomously controlled vehicle (ACV or ego vehicle) and other object vehicles (OVs) are model-predicted for the duration of the prediction horizon based on the current measurements. This allows the ACV to assess the risk of having a collision with other OVs and then to determine a collision-free trajectory. Different models used for motion prediction of OVs are summarized in [25], including physics-based models, maneuver-based models, and interaction-aware models. Physics-based models [26], [27] simply assume constant velocity or constant accelerations and thus they can only be used in motion prediction for a short-term (less than 1 second). Maneuver-based models [28], [29] predict the motion based on the estimation of maneuver intentions. Interaction-aware models [30], [31] also consider the inter-dependencies between the individual vehicles' maneuvers. The latter two models allow longer-term prediction compared to physics-based models. The interaction-aware model is more reliable than maneuver-based models, but it's also much-more computationally expensive, difficult to fully characterize, and is not compatible for real-time risk assessment [25]. Maneuver-based models remain the viable options for real-time long-term motion prediction (more than a second).

The planning problem naturally involves uncertainties due to modeling errors, sensor imperfections, or environmental disturbances, as summarized in [32]. In prediction of the motion of the OVs for risk assessment, the uncertainties can be handled by either using robust reachability analysis [33]–[36] (estimating the propagation of the uncertainty bounds) or using stochastic reachability analysis [37], [38] (estimating the propagation of the uncertainty distribution). In the reachability analysis case, the worst case of the uncertainty is considered thus leading to a very conservative solution for the planning problem. However, for stochastic reachability analysis, the reachable set as well as the risk of collision can be assessed by probabilities. If the state uncertainties are Gaussian

distributed, the stochastic reachability analysis can be implemented via filtering techniques, e.g., Kalman filter (KF) series [39], [40] for motion prediction of one maneuver and Interactive Multi Model (IMM) KF or Switching KF [41] for different possible maneuvers. Therein, the computational process for solving for the collision-free trajectory of the ACV in the MPC with filtering techniques is similar to applying stochastic reachability analysis applied to find a fail-safe trajectory [38].

Also, due to the sub-optimality caused by the nonconvex configuration space, an ACV with static or pre-configured optimization setups could get trapped at undesired local minima. Therefore in [42], a predictive control framework which can switch from a combination of rule-based discrete maneuver decisions is applied. With these rule-based decisions, the planned trajectories can be forced out of undesired local minima. Later in [43], to improve the optimality of the maneuver decisions, the lane selection and the related desired speed selection on the lane, is integrated within the optimization problem. To transform the resulting mixed-integer nonlinear programming problem (MINP) into a regular nonlinear programming (NLP) problem for real-time implementation, we proposed a relaxation method. However, in [43], only one maneuver can be selected for the whole prediction horizon. Furthermore, in the limited work presented there, measurement noise and other uncertainties were not considered in the problem formulation.

The present paper builds on the above with the following additional contributions: 1) The maneuver selection is extended from searching for one optimized maneuver for the entire prediction horizon to solving for an *optimized sequence of maneuvers* for the prediction horizon. Therein, a predictive reference speed assignment and adjustment strategy is proposed to pre-plan the longitudinal motion and to force the optimization solver "jump" out of undesired minima. 2) Here, we explicitly include uncertainties in the estimation and prediction of the states of the ACV and of the OVs as well as in determining the evolution of the tightened MPC constraints to explicitly accommodate uncertainties. 3) We include a computational complexity analysis of the naive MINP formulation as well as of the proposed relaxation technique for the specific active set solver adopted. 4) We compare the performance of the proposed optimized maneuver sequence planning with the one optimized maneuver approach under extended simulations that covers several complex scenarios on a highway.

The rest of the paper is organized as follows. Section II introduces the overall control framework. Section III describes the vehicle model of the ACV and the OV subject to sensing uncertainty and filtering techniques for state estimation and prediction. The hybrid system modeling of the vehicle maneuvers as well as the rule-based reference speed automaton are given in Section IV. Section V describes the formulation of MPC for maneuver and trajectory planning, the relaxation method proposed to transform the MINP to NLP and the reduction of the computational complexity due to the proposed relaxation. Simulations results and corresponding discussions are included in Section VI to illustrate the workings
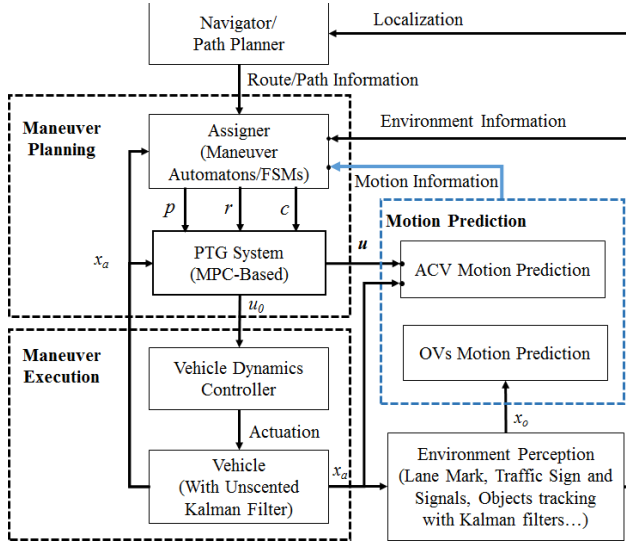
This article has been accepted for inclusion in a future issue of this journal. Content is final as presented, with the exception of pagination.

WANG *et al.*: PREDICTIVE MANEUVER PLANNING FOR AN AUTONOMOUS VEHICLE IN PUBLIC HIGHWAY TRAFFIC

3

Fig. 1. Hierachical control framework.

Fig. 2. Particle motion description for the vehicle.

of the proposed framework. Conclusions are offered in Section VII.

II. CONTROL FRAMEWORK

Figure 1 shows a schematic of the proposed predictive maneuver planning and control framework for an autonomous road vehicle in a uncertained public traffic environment. At the top the assigner module integrates/fuses the information from the environment perception module (lane detection, traffic sign and signals, object tracking...), the navigator/path planner module (route navigator for on-road situation and path planner for off-road situation), the vehicle dynamics sensing/estimation modules (planer and yaw motion of the ACV) and motion prediction module (both ACV and tracked OVs). Here, we assume the states of the ACV x_a and OV x_o are fully observed/estimated. The fused information will be provided to some pre-defined finite state machines (FSMs)/maneuver automatons and then the decisions on configurations, e.g., parameters (p), references (r), and constraints (c), for the MPC formulation will be made and assigned to the predictive trajectory guidance (PTG) module. Further description of these can be found in [19] and will be also briefly mentioned in Section III.

The maneuver automatons/FSMs designed and stored in the assigner module are scenario-based. Once the possible maneuvers for a scenario are captured, like cruising, following, leading and lane change for highway scenario [44] (see Figure 4), or going left/right/straight and stop for intersection scenario [45], the relevant FSM can be easily extended for the same scenario or to other scenarios [46]. The candidate maneuvers in the FSMs are related to their own references, e.g. desired speed and lane. At each prediction interval of the MPC, the references are pre-selected according to the predicted motion of the ACV and the surrounding OVs via filtering techniques. Then, the optimized maneuver sequence as well as the optimized relevant control output trajectory u for the whole horizon are solved simultaneously by the PTG
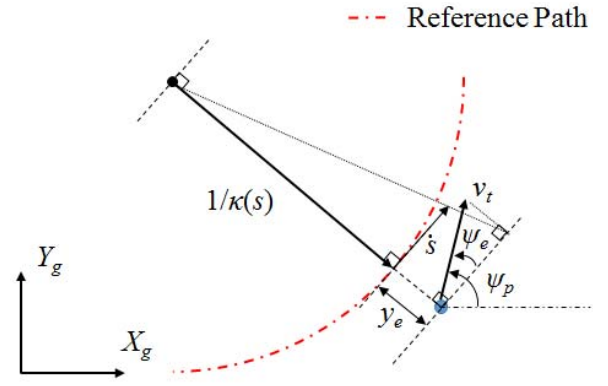
system, according to the objective function and constraints to be detailed later. When the maneuver planning is done, the first interval of u, i.e., u_0 is sent to the lower-level controllers of the continuous vehicle dynamics for execution via the available lower-level vehicle dynamics controllers (VDC). The lower-level controllers are responsible for manipulating the available actuators like electronic throttle, braking actuators or electric steering motors so as to track the desired longitudinal and lateral acceleration signals generated by the upper-level PTG system. The reader is referred to [19], [47] and other standard references for this topic.

III. VEHICLE MODELS AND FILTERING DESIGN

A. Particle Motion Based Vehicle Model

The use of a 2D curvilinear particle motion model in the Frenet frame (see Figure 2) for vehicle motion description in trajectory planning has been detailed in previous works [19], [48]. The reasons we adopted this model include: 1) it is simple enough to use and implement for real-time computations, 2) it describes the kinematic planar motion of an object like a car well, 3) we can incorporate road curvature information directly in the model; thus, it is suitable for path tracking problems. For convenience, we shall present here the continuous time models of the state dynamics even if computations are ultimately to be done in discrete time form. Adding process uncertainties (random disturbances and uncertainties) and measurement noise, the nonlinear dynamic model describing the motion of the ACV can be written as:

$$
\begin{bmatrix} \dot{v}_t \\ \dot{\psi}_e \\ \dot{s} \\ \dot{y}_e \\ \dot{a}_t \\ \ddot{\psi}_p \end{bmatrix} = \begin{bmatrix} a_t \\ \dot{\psi}_p - v_t \cos(\psi_e)\kappa(s)/[1 - y_e\kappa(s)] \\ v_t \cos(\psi_e)/[1 - y_e\kappa(s)] \\ v_t \sin(\psi_e) \\ -a_t/T_{a_t} \\ [v_t\kappa(s) - \dot{\psi}_p]/T_{\dot{\psi}_p} \end{bmatrix}
$$
$$
+ \begin{bmatrix} 0 & 0 \\ 0 & 0 \\ 0 & 0 \\ 0 & 0 \\ 1/T_{a_t} & 0 \\ 0 & 1/T_{\dot{\psi}_p} \end{bmatrix} \begin{bmatrix} a_{t,d} \\ \Delta\dot{\psi}_{p,d} \end{bmatrix} + \begin{bmatrix} 0 & 0 \\ 0 & 0 \\ 0 & 0 \\ 0 & 0 \\ 1 & 0 \\ 0 & 1 \end{bmatrix} \begin{bmatrix} w_{a_t} \\ w_{\Delta\dot{\psi}_d} \end{bmatrix}
$$

This article has been accepted for inclusion in a future issue of this journal. Content is final as presented, with the exception of pagination.

4

IEEE TRANSACTIONS ON INTELLIGENT TRANSPORTATION SYSTEMS

$$
\begin{bmatrix} y_s \\ y_{y_e} \\ y_{a_t} \\ y_{\dot{\psi}_p} \end{bmatrix} = \begin{bmatrix} 0 & 0 & 1 & 0 & 0 & 0 \\ 0 & 0 & 0 & 1 & 0 & 0 \\ 0 & 0 & 0 & 0 & 1 & 0 \\ 0 & 0 & 0 & 0 & 0 & 1 \end{bmatrix} \begin{bmatrix} v_t \\ \psi_e \\ s \\ y_e \\ a_t \\ \dot{\psi}_p \end{bmatrix}
$$
$$
+ \begin{bmatrix} 1 & 0 & 0 & 0 \\ 0 & 1 & 0 & 0 \\ 0 & 0 & 1 & 0 \\ 0 & 0 & 0 & 1 \end{bmatrix} \begin{bmatrix} v_s \\ v_{y_e} \\ v_{a_t} \\ v_{\dot{\psi}_p} \end{bmatrix} \tag{1}
$$

where v_t, a_t and $\dot{\psi}_p$ are, respectively, the absolute forward speed, forward acceleration and yaw rate of the vehicle. ψ_e, s and y_e are, respectively, the angular alignment error, arc length and lateral position error of the vehicle with respect to the reference path coordinate. The reference path is defined by its curvature $\kappa(s)$ in terms of the arc length s. $\kappa(s)$ can be captured by interpolating curves, e.g., polynomial curves by lane detection [20], [21] from perception module or from a path planning module [11]. In addition, assuming the (lower-level) closed-loop vehicle dynamics exhibits a first-order lag behavior, the generation of a_t and $\dot{\psi}_p$ can be approximated by a first-order dynamics system with additive Gaussian process noise $w = [w_{a_t} w_{\Delta \dot{\psi}_d}]$. This process noise is used to model disturbances (e.g. wind, road, unmolded dynamics) affecting the longitudinal and lateral dynamics of the ACV. T_{at}, $T_{\dot{\psi}_p}$ are the time-constants of the first-order approximation of the longitudinal and lateral dynamics of the vehicle (masked by available VDC). Here, the desired forward acceleration $a_{t,d}$ and the desired deviation from the reference yaw rate $\Delta \dot{\psi}_{p,d}$ are treated as the final inputs used to control the vehicle/particle along the reference path. The use of $\Delta \dot{\psi}_{p,d}$ facilitates the computation of smooth inputs since known reference curvature information is already taken into account (see [19]). For the system outputs, we consider that the available measurements are positions s, y_e (e.g., from GPS) and the inertial states a_t, $\dot{\psi}_p$ (e.g., from IMU) with assumed Gaussian sensor noise $v = [v_s v_{y_e} v_{a_t} v_{\dot{\psi}_p}]^T$.

For an OV, its motion is also defined in the Frenet frame as a particle. To consider its maneuver intention for better motion prediction, we assume each OV to follow closed-form dynamics that describe longitudinal motion like cruising at a specific speed or speed change and lateral motion like tacking a specific lane or lane change. One possible form is:

$$
\begin{bmatrix} \dot{s}_o \\ \dot{v}_{t,o}^s \\ \dot{y}_{e,o} \\ \dot{v}_{n,o}^s \end{bmatrix} = \begin{bmatrix} 0 & 1 & 0 & 0 \\ 0 & \dfrac{-K_{s1}}{1+K_{s2}} & 0 & 0 \\ 0 & 0 & 0 & 1 \\ 0 & 0 & -K_{y1} & -K_{y2} \end{bmatrix} \begin{bmatrix} s_o \\ v_{t,o}^s \\ y_{e,o} \\ v_{n,o}^s \end{bmatrix}
$$
$$
+ \begin{bmatrix} 0 & 0 \\ \dfrac{K_{s1}}{1+K_{s2}} & 0 \\ 0 & 0 \\ 0 & K_{y1} \end{bmatrix} \begin{bmatrix} v_{t,o,ref}^s \\ y_{e,o,ref} \end{bmatrix}
$$

$$
+ \begin{bmatrix} 0 & 0 \\ \dfrac{1}{1+K_{s2}} & 0 \\ 0 & 0 \\ 0 & 1 \end{bmatrix} \begin{bmatrix} w_{\dot{s},o} \\ w_{y,o} \end{bmatrix}
$$
$$
\begin{bmatrix} y_{s_o} \\ y_{y_{e,o}} \end{bmatrix} = \begin{bmatrix} 1 & 0 & 0 & 0 \\ 0 & 0 & 1 & 0 \end{bmatrix} \begin{bmatrix} s_o \\ v_{t,o}^s \\ y_{e,o} \\ v_{n,o}^s \end{bmatrix} + \begin{bmatrix} 1 & 0 \\ 0 & 1 \end{bmatrix} \begin{bmatrix} v_{s,o} \\ v_{y,o} \end{bmatrix} \tag{2}
$$

where, s_o and $y_{e,o}$ are the arc length and lateral position error of the OV; $v_{t,o}^s$ and $v_{n,o}^s$ are the tangential speed and normal speed of the OV along its reference lane. K_{s1} and K_{s2} are the proportional and integral gains of a controlled OV tracking the reference speed $v_{t,o,ref}^s$ with assumed Gaussian process noise $w_{\dot{s},o}$. K_{y1} and K_{y2} are the proportional and integral gains of a controlled OV tracking its reference lane $y_{e,o,ref}$ with assumed Gaussian process noise $w_{y,o}$. These gains can be identified from the human-driver data to emulate different driving habits, e.g. either aggressive or conservative [49]. For system outputs, only the positions s_o and $y_{e,o}$ are assumed measured with associated Gaussian sensor noises $v_{s,o}$ and $v_{y,o}$ (e.g., from on-board range sensors like radars on the ACV).

B. Filtering Design for Motion Estimation and Prediction

Given the nonlinear system model in (1), we adopt Unscented Kalman Filter (UKF) [50] to estimate the motion states of ACV in the presence of process and measurement uncertainty/noise. Given the linear dynamics motion models for the OVs (2), a regular KF can be used for state estimation of one maneuver (tracking a specific lane and speed). To account for other possible maneuvers of the OVs, the Inter-active Multi-Model KF algorithm [41], [51] can be applied for OV state estimation. Here, we assume the gains are well captured from the driving data for the drivers of all OVs of all maneuvers.

Given the current estimates of the ACV and OV states, one can predict the evolution of the mean and covariance of the states for the whole length of the prediction hori-zon of the MPC. Here, we propagate uncertainty in the predicted states (for both ACV and OV) using the filtering techniques(UKF/KF) based on (1) and (2) with the notion of the most likely measurement. This notion is based on the assumption that the future measurements in the update of the filter recursions are approximated well by the prediction. This assumption is motivated by the fact that future measurements are unavailable. Even though the updated covariance is not directly affected by the value of the measurement, as the mea-surement information is considered (via the only assumption that same sensors and models are to be used), the uncertainties in the likely state are reduced. It is shown in [39] that the most likely measurement will not introduce bias in the system, thus it is useful to constrain the uncertainty propagation. Finally, note that the future inputs used in the motion prediction of the ACV will be taken from the previous planning results of the MPC.

This article has been accepted for inclusion in a future issue of this journal. Content is final as presented, with the exception of pagination.

WANG *et al.*: PREDICTIVE MANEUVER PLANNING FOR AN AUTONOMOUS VEHICLE IN PUBLIC HIGHWAY TRAFFIC 5

The above models for motion prediction of OVs and the ACV do not explicitly consider the interactions between vehicles, particularly those that would exist in mixed-traffic involving other human-driven vehicles. As alternatives, other motion prediction approaches such as interactive multi-model filtering, Bayesian Networks, and Hidden Markov Models trained on human-driver data are all possible options [31], [52]. While any of these approaches may be used for motion prediction and incorporated with the maneuver planning framework presented in this paper, as we point out later, for multiple OVs in multi-lane scenarios, the computational complexity of using even linear motion models for the OVs needs to be handled with care.

IV. HYBRID SYSTEM MODELING OF THE VEHICLE MANEUVERS AND RULE-BASED REFERENCE SPEED AUTOMATON

A. Hybrid System Modeling of the Vehicle Maneuvers

The hybrid system notion is straightforward to apply to the motion of a road vehicle, since basic maneuvers, like accelerating, cruising or decelerating in the longitudinal direction and steering to the left or right in the lateral direction can be identified from the vehicle's motion [44], [45]. For the ACV, these maneuvers can be designed via tracking different reference speeds and reference paths/lanes [42]. This results in a hybrid system model involving tracking of *two-dimensional* discrete references (speed and lane) and the underlying continuous vehicle motion trajectories. To reduce the complexity of the maneuver planning for a prediction horizon, the switching among the discrete references can be done hierarchically (see Figure 3, for example): 1) Firstly, the switching of the reference speeds assigned for each lane based on pre-defined rules (rule-based switch sets) is executed at each prediction step in the horizon. This is called rule-based switch. 2) Then, an optimization problem is solved for the whole horizon to find the optimized switching sequence for the reference lanes. This is called optimization-based switch. For different scenarios, the maneuvers and the rule-based switch sets can be specifically designed and stored in different FSMs of the assigner module, e.g., single lane, intersection, etc.

B. Rule-Based Reference Speed Automaton

1) Reference Speed Assignment: Considering the interaction of the vehicle with the surrounding dynamic environment, e.g. the traffic sign, signals and OVs, for example, when approaching a slow front OV, a normal reaction of the vehicle will be either slowing down to follow it or simply changing lane to overtake it. Those intentions can be reflected by the reference speed assignment to the ACV. Specifically, on lane l, a relevant reference speed $v_{t,r,l}$ will be assigned to the ACV to follow, depending on the detection of approaching or close by object vehicles, as shown in Figure 4. The detection condition (3) and approaching condition (4) are defined by:

$$\left| \hat{s} - \hat{s}_{o_i} \right| < T_d v_{t,ref} \tag{3}$$

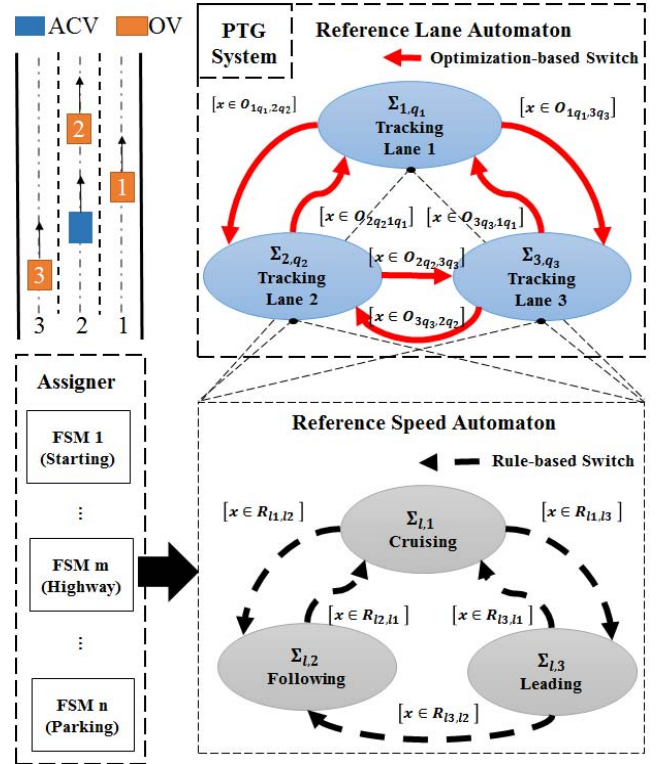$$\left(\hat{s} - \hat{s}_{o_i} \right) \left(v_{t,ref} - \hat{v}_{t,o_i}^s \right) < 0 \tag{4}$$

Fig. 3. Maneuver automaton example for 3-lane highway scenario. Rule-based switch sets are denoted by R.

where T_d is the detection preview time (set from specifications of the perception module, its value should be larger than the predictive horizon H_p to prevent the ignorance of an abrupt event from the surrounding traffic for MPC). Here, and in the following, the usual hat (^) notation is used to denote the respective estimated states. The ith OV occupying lane l is denoted by:

$$\hat{y}_{e,o_i} \in \left[\underline{y_{e,l}}, \overline{y_{e,l}} \right] \tag{5}$$

where $y_{e,oi}$ is the lateral position of OV i in the path coordinate and the lane l is demarked by the lateral position bounds $\left[\underline{y_{e,l}}, \overline{y_{e,l}} \right]$.

Accordingly, the cruising maneuver is defined as tracking a desired cruise speed $v_{t,ref}$ on lane l (lane 2 in Figure 4) without detecting any approaching OVs on the same lane. The corresponding speed relation and reference speed assignment is given by:

$$v_{t,r,l} = v_{t,ref} \tag{6}$$

The following or leading maneuver refers to tracking the speed $v_{t,oi}^s$ of a detected approaching OV on lane l in the front or rear by assigning:

$$v_{t,r,l} = \hat{v}_{t,o_i}^s \tag{7}$$

2) Reference Speed Adjustment: Generally, the ACV is expected to track the desired cruise speed $v_{t,ref}$ within the acceptable speed range $[v_{t,cl}, v_{t,ch}]$ with positive speed
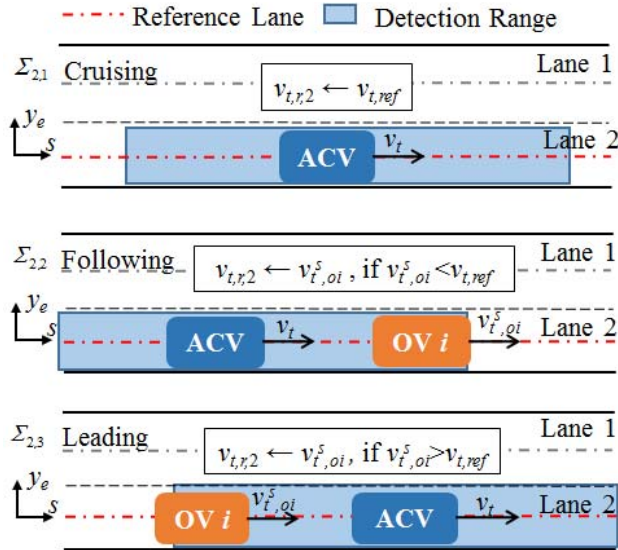
This article has been accepted for inclusion in a future issue of this journal. Content is final as presented, with the exception of pagination.

6

IEEE TRANSACTIONS ON INTELLIGENT TRANSPORTATION SYSTEMS

Fig. 4. Reference speed assignment for ACV in 2 lane scenario.

Fig. 5. Prediction of reference speed assignment and adjustment.

tolerance Δv_t:

$$\begin{cases} v_{t,cl} = v_{t,ref} - \Delta v_t \\ v_{t,ch} = v_{t,ref} + \Delta v_t \end{cases} \tag{8}$$

However, as argued in [43], by following the optimization-based reference lane automaton introduced in the next section, the ACV can be "trapped" in one lane in a following or leading maneuver due to the formulation of MPC objective function with a lane selection variable (to be described later). In such situations, a forced lane change is necessary to help the ACV jump out of the trap. Therefore, we extend the rules used in [42] to guide the ACV to an adjacent empty lane or to one with the assigned speed closest to the desired cruise speed via reference speed adjustment. If the assigned reference speed of the ACV in the current lane l goes outside of this speed range:

$$\hat{v}_{t,r,l} \notin [v_{t,cl}, v_{t,ch}] \tag{9}$$

and adjacent lane(s) are unoccupied or are with assigned speeds closest to $v_{t,ref}$, with complementary sets defined by:

$$\left| \hat{s} - \hat{s}_{o_{tl}} \right| < d_s \text{ or } \hat{v}_{t,r,l\pm1} \notin [v_{t,cl}, v_{t,ch}]$$
$$\text{or } \left| \hat{v}_{t,r,l\pm1} - v_{t,ref} \right| = \min \left| \hat{v}_{t,r,i} - v_{t,ref} \right|, \quad i = [1, \ldots, N_l] \tag{10}$$

then a forced lane change will be assigned. Here, d_s is a safe headway distance between the ACV and the preceding OV which will be defined in the next section (see equation (13)). A forced lane change is activated by adjusting the assigned speed for those lanes with following or leading maneuver outside the acceptable speed range. The adjustment is given by:

$$v_{t,r,j} = k_l \hat{v}^s_{t,o_j}, \ \hat{v}^s_{t,o_j} \notin [v_{t,cl}, v_{t,ch}], \quad k_l \in \left[0, \frac{v_{t,\max}}{\hat{v}^s_{t,o_i}}\right] \tag{11}$$

where k_l is the adjustment factor and $v_{t,\max}$ is the maximum speed of the ACV. k_l can be selected to generate a high value of the objective function associated with tracking the
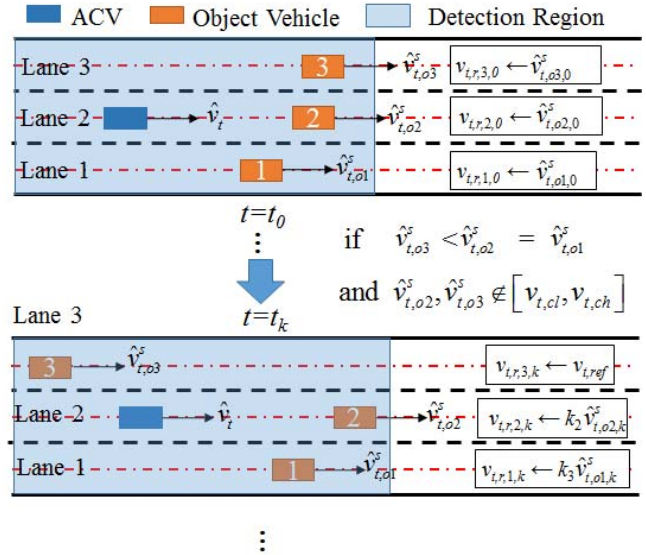
TABLE I
CONFIGURATION OF THE RULE-BASED REFERENCE
SPEED AUTOMATON FOR LANE l

Switch Set	Rule Description
$R_{l1,l2}$	(3)∩(4)∩(5)
$R_{l2,l1}$	$(3)^C$∪$(4)^C$ or (9)∪(10)
$R_{l1,l3}$	(3)∩(4)∩(5)
$R_{l3,l1}$	$(3)^C$∪$(4)^C$ or (9)∪(10)
$R_{l3,l2}$	(3)∩(4)∩(5)

adjusted reference speed of specific lanes. This will then force the MPC to track other lanes with closer assigned reference speed to the desired cruising speed $v_{t,ref}$ with lower values of the objective function. An example of the reference speed assignment and adjustment for multiple-lane scenario is shown in Figure 5.

In summary, the configurations of rule-based reference speed automatons for FSMs are listed as in Table I. In the rule description, the symbol "∩" represents intersection, "∪" means union, and the superscript "C" represents complement.

Remark 1: Given a prediction horizon of length N_p steps, the rule-based reference speed automaton of Table 1 is applied for every lane at every prediction interval. This means a reference speed sequence with N_p elements will be generated for each lane, thus effectively constructing a *two-dimensional pre-plan* of the references in both the longitudinal and lateral directions. This will be used later in the MPC to find the best sequence of reference selections for the whole horizon that minimize an objective function. Note that there is a possible loss of performance from the non-optimality of the reference speed assignment rules; but these are discrete rules executed outside of the MPC; the optimization of such assignment rules is beyond the scope of our paper.
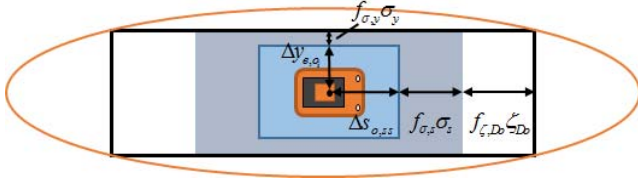
This article has been accepted for inclusion in a future issue of this journal. Content is final as presented, with the exception of pagination.

WANG *et al.*: PREDICTIVE MANEUVER PLANNING FOR AN AUTONOMOUS VEHICLE IN PUBLIC HIGHWAY TRAFFIC 7

Fig. 6. Elliptical boundary for collision avoidance with combined uncertainties σ_s, σ_y of ACV and OV.

V. MPC-BASED LANE SELECTION AND TRAJECTORY PLANNING

We configure the MPC in this section with the ability to conduct predictive lane change maneuver planning and guidance, with advance knowledge of the predicted reference speed assignment as described above.

A. Tightened Collision Avoidance Constraints

The constraint to keep a safe distance between the ACV and any nearby OV i with the predicted uncertainties is tightened by the following elliptic inequality:

$$\left(\frac{y_e - \hat{y}_{e,o_i}}{\Delta y_{e,o_i} + f_{\sigma,y}\sigma_y} \right)^2 + \left(\frac{s - \hat{s}_{o_i}}{d_s} \right)^2 \geq 1 \quad (12)$$

$$d_s = \Delta s_{o,ss} + f_{\sigma,s}\sigma_s + f_{\zeta,Do}\zeta_{Do} \quad (13)$$

This constraint is depicted in Figure 6. A rectangular region is inscribed in the ellipse. Its dimensions $\Delta y_{e,oi}$ and $\Delta s_{o,ss}$ are calculated by incorporating the geometry (length and width) of OV i and the ACV. $\sigma_s = \sigma_{s,ACV} + \sigma_{s,oi}$ and $\sigma_y = \sigma_{y,ACV} + \sigma_{y,oi}$ are the combined covariances of, respectively, the arc length and lateral position error of ACV and OV i, based on the predicted covariances from the motion prediction module. Multipliers $f_{\sigma,s}$ and $f_{\sigma,y}$ define the cross-belief region of the combined states. For example, $f_{\sigma,s} = f_{\sigma,y} = 3$ approximates a cross-belief region with belief coefficient $\delta = 99\%$ between the arc length and lateral position. ζ_{Do} is a slack variable used to define a speed-based headway distance between the ACV and OV that can extend the collision area of an OV (tightening the avoidance constraints, see equations (12) and (13), and Figure 6). The variable can be used to obtain conservative and comfortable responses. For example, in an emergency situation with an OV executing a sudden cut-in lane change, the MPC solver for the ACV can pursue hard braking/speed reduction by further reduction of the variable ζ_{Do} thereby reducing the headway space/distance. This expands the feasible space for the solver that can be used in situations like this. See [19] for detailed discussions of this. We give it the auxiliary dynamics:

$$\dot{\zeta}_{Do} = u_{\zeta_{Do}} \quad (14)$$

In (13), $f_{\zeta,Do}$ is an tuning parameter (has a unit of time, typically $f_{\zeta,Do} > T_{mpc}$). To ensure a safety headway distance (exclude extreme events between MPC update intervals T_{mpc}) the following constraint should be satisfied:

$$\zeta_{Do} \geq T_{mpc}v_t/f_{\zeta,Do} \quad (15)$$

Other state constraints like friction ellipse of a real vehicle's tire/road contact, lane boundaries, speed limits and the minimum turning radius, etc. are also considered with uncertainties, for complete details, please refer to [19].

B. MPC Problem Formulation

As uncertainties are considered, the lane selection maneuver planning problem to be solved over the prediction horizon $[0, H_p]$ results in a stochastic MPC problem that is formulated by:

$$\min_{x_k, u_k} E \left(\sum_{k=1}^{N_p} \sum_{l=1}^{N_l} \| z_{l,k} (y_{1,k} - r_{1,l,k}) \|_{P_1}^2 \right.$$
$$\left. + \sum_{k=1}^{N_p} \| y_{2,k} - r_{2,k} \|_{P_2}^2 + \sum_{k=0}^{N_p-1} \| u_k \|_R^2 \right) \quad (16)$$

subject to : $\dot{x} = f(x, u, w), \quad x \in X, \ u \in U, \ w \in W$ (17)

$$x(0) = x_0 \quad (18)$$

$$\sum_{l=1}^{N_l} z_l = 1, z_l \in \{0, 1\}, \quad \forall l \in \{1, \ldots, N_l\} \quad (19)$$

$$\Pr(c_1(x, u) \geq 0) \geq \delta \quad (20)$$

$$c_2(x, u) \geq 0 \quad (21)$$

Here, the cost function minimizes the expectation of state tracking error and control efforts. x covers all the state variables of the ACV particle motion model given by (1), the slack variables in (14) and lane selection variables $z_1 \sim z_{Nl}$ whose dynamics is described below in (23). X represents the state-space for x. x_0 denotes the current/initial state (measured and estimated). The estimation of the system outputs, namely the speed v_t and lateral position y_e of the ACV are grouped in vector y_1, and the slack variable outputs ζ_{Do} is in y_2. $r_{1,l}$, r_2, are, respectively, the candidate output references for lane l and references for the slack variables (corresponding respectively to y_1 and y_2). P_1, P_2 and R are the weighting matrices for the candidate maneuver tracking error, slack variable reference tracking error and control efforts, respectively. In (17), U denotes the admissible set for input u, which includes the input to ACV motion model and selection variables. W is the state space for noise/disturbance w defined in (1). The continuous model (17) is eventually discretized in sample steps ΔT, $\Delta T = H_p/N_p$ and H_p is the horizon length.

The collision avoidance constraints are written compactly as equation (20) with a nonlinear vector function c_1 and are considered to be generally probabilistic with a belief coefficient δ. For computing solutions efficiently, these constraints are eventually converted (tightened) into conservative deterministic constraints such as those we have already written as (12). In (12), multipliers $f_{\sigma,s}$, $f_{\sigma,y}$ can be written in a function of δ based on accumulated Gaussian distributions for the respective states [39], [51]. Similarly, the vector function c_2 in (21) is a compact representation of other deterministic inequality constraints like the tire-road friction ellipse or speed limits, or headway safety distance (15), etc.

In order to realize the optimization-based lane selection, we utilize a suite of selection variables z_l that take on

This article has been accepted for inclusion in a future issue of this journal. Content is final as presented, with the exception of pagination.

8

IEEE TRANSACTIONS ON INTELLIGENT TRANSPORTATION SYSTEMS

binary (integers 0 or 1) values (with their summation equal to 1 for each time step) in (19) to coordinate the consideration of tracking different lanes and their corresponding assigned reference speeds (by the pre-planning described in the previous section). However, this formulation leads to a MINP problem and it's hard to solve at real time. Therefore, we apply an approximation method we proposed in [43] (and described futher in Remark 2 below) to relax the original MINP problem, where the the integrality constraint in (19) is replaced with the following relaxed formulation (22):

$$\sum_{l=1}^{N_l} z_l = 1, \quad z_l \in [0, 1], \quad \forall l \in \{1, \ldots, N_l\} \quad (22)$$

Here, with the relaxed formulation (22), the selection variables z_l are regarded as additional continuous states with the auxiliary dynamics (included among the state equations in (17)):

$$\begin{cases} \dot{z}_l = u_{z_l}, & \text{if } l \neq N_l \\ \dot{z}_l = -\sum_{i=1}^{N_l-1} u_{z_i}, & \text{if } l = N_l \end{cases} \quad (23)$$

Remark 2: To solve a MINP problem efficiently at real time, two fundamental approximation methods can be applied in tandem: relaxation and constraint enforcement [53]. The relaxation approach is to extend the feasible solution set of the problem, by relaxing or neglecting certain constraints, e.g., relaxing the integrality constraint from (19) to (22). Afterward, constraint enforcement can be sought to exclude the solutions that are feasible under the relaxation but not for the original problem. For our problem formulation, the constraint enforcement is deemed optional as the relaxation of the integrality constraint will not affect the global minimum of (16). The optimization will naturally converge to tracking only one of the lanes if the configuration space is convex. If it is not, we have the following case.

Remark 3: With the relaxation of the lane selection variable involved in the integrality constraint, the ACV is no longer strictly guided to track only one of lanes. This may lead to undesired behaviors of the ACV in complex traffic scenarios with few available lanes, where the ACV may laterally approach an adjacent OV and stay in between two lanes until the OV is overtaken, as shown in our previous results [43]. More rules designed in the reference speed automaton for these situations may help to improve or exclude such behavior. The proposed rule-based speed assignment over the whole prediction horizon is meant to address this issue.

C. Computational Complexity

The computational complexity of our MPC formulations can be estimated. For our purposes, we solved the nonlinear programming problem above using the ACADO (Automatic Control and Dynamic Optimization) Toolkit [54] which implements qpOASES, a one-iteration SQP algorithm employing an active set strategy. From [55], the computational complexity of solving the MPC problem for tracking only one reference lane and reference speed with a prediction horizon length N_p
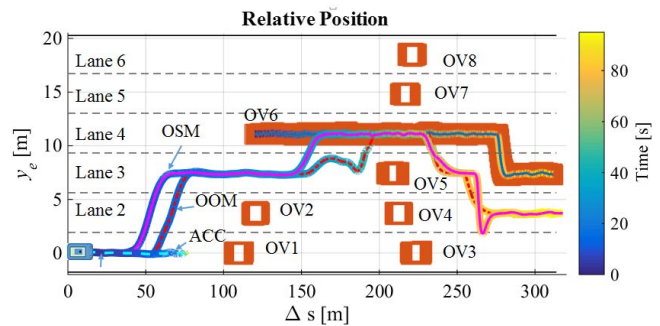

Fig. 7. Relative position of ACV and OVs in the simualtion.

is at most $O(g(N_x, N_u, N_p, N_c))$, where:

$$g\left(N_x, N_u, N_p, N_c\right) = N_x^3 + N_u^2 + N_p^2 + (N_u N_p)^2 + N_c N_u N_p \quad (24)$$

which is in low-order polynomial time. Here, N_x is the number of states, N_u is the number of control inputs, N_p is the length of the prediction horizon, N_c is the number of constraints. The computational complexity of solving the MINP problem is then $(N_l^{N_p} g(N_x, N_u, N_p, N_c))$, which is in high-order polynomial time, since N_p is typically in the order of 40 or more for the present application. The computational complexity of the resulting NLP problem with the approximation method is at most $O(g(N_x + N_l, N_u + N_l - 1, N_p, N_c + N_l + 1))$, which is in low-order polynomial time. Therefore, by adopting the approximation method, the complexity of solving the MINP problem can be significantly reduced to an NLP problem with much less computational burden. As we comment in the next section, the resulting execution times are feasible for real-time implementation in the many scenarios we have tested.

VI. RESULTS AND DISCUSSIONS

A. Simulation Settings

To illustrate the performance of the predictive maneuver planning approach, we consider a straight six-lane highway where the ACV faces sequentially connected scenarios, like overtaking, following and collision avoidance in the presence of eight nearby object vehicles (OVs), as shown in Figure 7. The situations progress from those requiring simple responses (lane change) to aggressive ones that push the vehicle dynamics and the control to the limit. The proposed approach, hereafter labeled OSM (for optimized sequence of maneuvers within a prediction horizon), will be compared with the previous approach in [43] where only one optimized maneuver (labled OOM) is selected for the entire prediction horizon. We also compare the results to a common adaptive cruise control (ACC) scheme to show the advantage of two-dimensional maneuver planning. The assumed uncertainties for the ACV and OVs motion models are given in Table II, where the disturbances/noises are modeled by normal distribution $N(\mu, \sigma^2)$ with mean μ and covariance σ^2. The parameters selected for the MPC formulation are listed in Table III. The parameters in Table II and III are chosen based on experimental tuning. Details about tuning the MPC weights for one lane tracking
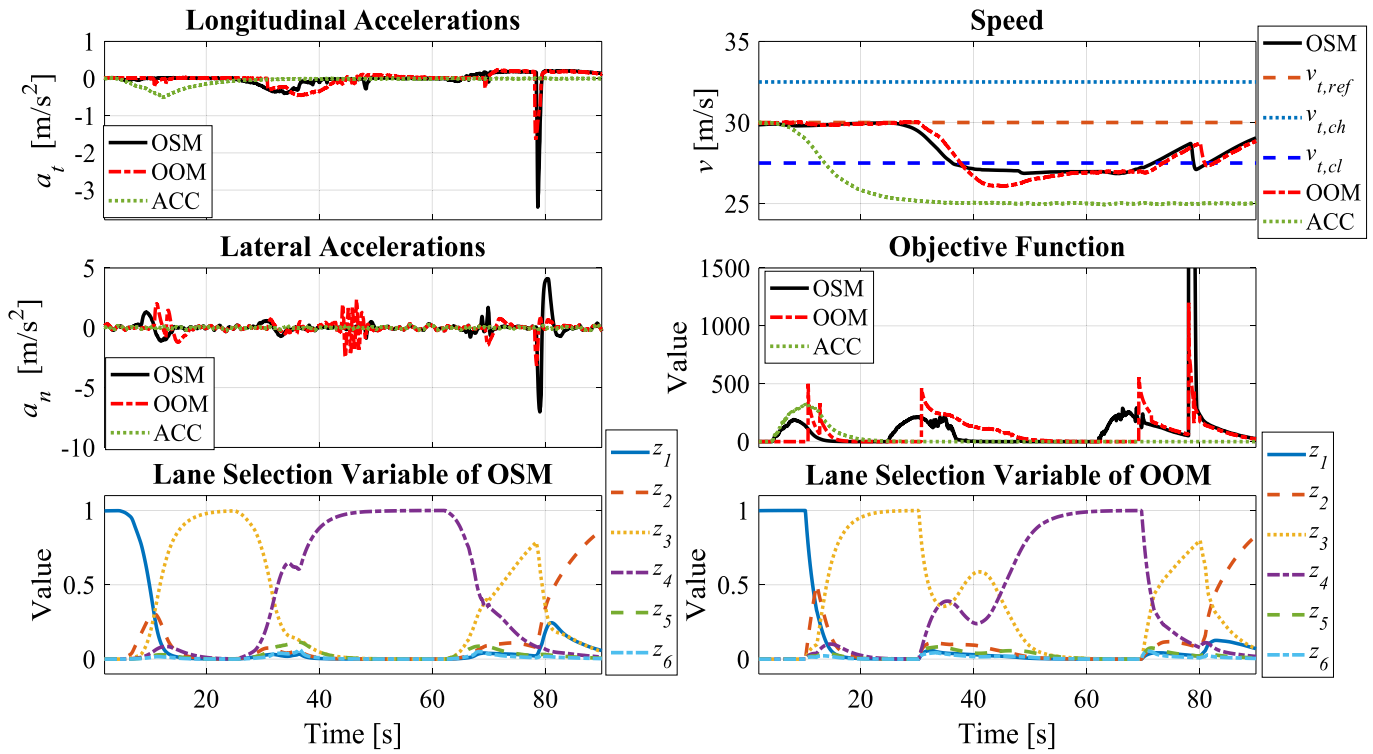
This article has been accepted for inclusion in a future issue of this journal. Content is final as presented, with the exception of pagination.

WANG *et al.*: PREDICTIVE MANEUVER PLANNING FOR AN AUTONOMOUS VEHICLE IN PUBLIC HIGHWAY TRAFFIC 9

Fig. 8. State evolutions for the whole duration under the different manuever planners and ACC.

TABLE II
UNCERTAINTIES AND PARAMETERS FOR ESTIMATION OF ACV AND OV

Vehicle	Parameter	Value	Vehicle	Parameter	Value
ACV	w_{a_t} [m/s²]	$N(0,0.01)$	OV (1~8)	$w_{s,o}$ [m/s]	$N(0,25)$
	$w_{\Delta\dot\psi_d}$ [rad/s²]	$N(0,10^{-4})$		$w_{y,o}$ [m]	$N(0,1)$
	v_s [m]	$N(0,0.01)$		$v_{s,o}$ [m]	$N(0,25)$
	v_{y_e} [m]	$N(0,0.01)$		$v_{y,o}$ [m]	$N(0,1)$
	v_{a_t} [m/s²]	$N(0,0.01)$		K_{s1}	2.5
	$v_{\dot\psi_p}$ [rad/s²]	$N(0, 10^{-4})$		K_{s2}	2
				K_{y1}	2.5
				K_{y2}	2

TABLE III
MAIN PARAMETERS SELECTED

Parameter	Value	Parameter	Value	Parameter	Value
$v_{t,ref}$ [m/s]	30	$\Delta s_{o,ss}$ [m]	5.3	$P_{2,\zeta_{gg}}$	20
Δv_t [m/s]	2.5	$\Delta y_{e,o_i}$ [m]	2.3	$P_{2,\zeta_{do}}$	20
Δy_e [m]	1.85	g [m/s²]	9.8	R_{a_t}	50
T_{at} [s]	0.075	N_p	40	$R_{\Delta\dot\psi_p}$	250
$T_{\psi p}$ [s]	0.2	ΔT [s]	0.15	$R_{u_{\zeta_{do}}}$	0.001
T_d	7s	k_v	0.8	$R_{u_{\zeta_{gg}}}$	0.001
$f_{\zeta,Do}$	0.5	$P_{1,ye}$	3	$R_{u_{zl}}$	100
$f_{\sigma,s}, f_{\sigma,y}$	3	$P_{1,vt}$	2		

were given in our recent paper [19]. However, in this paper, as several lanes are considered as candidates at the same time, additional weights on the lane selection control variables ($u_{zl}, l = 1 \sim N_l$) are introduced (and included in R). Tuning these weights is a trade-off between keeping the current lane and initiating a lane change when the lateral bias of the ACV is large. If the weights for u_{zl}, are high, the solution tends to keep the current lane; if the weights for u_{zl}, are set low, the solution will tend to make a lane change. The longitudinal speeds of the OVs are set to be constant at values to be discussed below for the various scenarios. The measurement sampling time/MPC update time T_{mpc} is set to 150ms.

B. Results and Discussion

The state trajectories for the whole scenario are shown in Figure 7 and Figure 8.

1) Preceding OVs Detected at Cruising (In the First 20 s): In this scenario, the ACV initially occupies lane 1 (right most lane) at its reference/desired speed of 30 m/s. Then, it faces two slower vehicles OV1 and OV2, going in parallel in lane 1 and lane 2 at speed of 25 m/s. At around time of 7 seconds, the ACV under OSM starts a lane change to lane 3, which is the closest available lane, to overtake OV1 and OV3. However, for the case with OOM, the lane change to lane 3 happens around 10 seconds. But the ACV

This article has been accepted for inclusion in a future issue of this journal. Content is final as presented, with the exception of pagination.

10

IEEE TRANSACTIONS ON INTELLIGENT TRANSPORTATION SYSTEMS
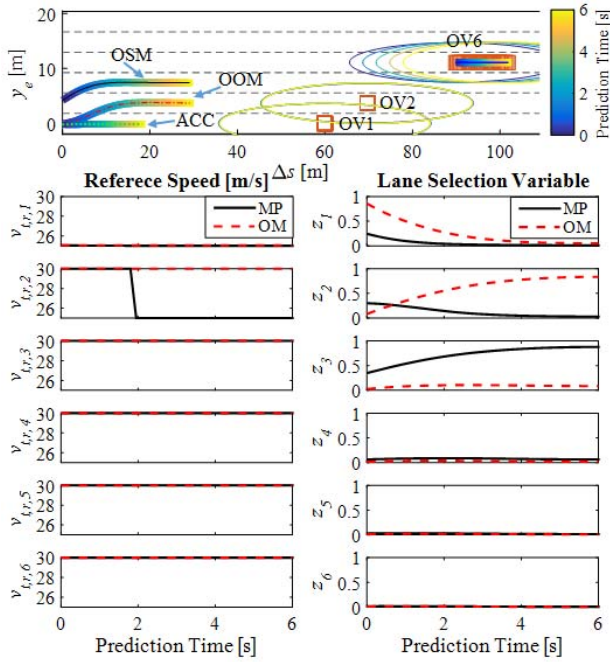
Fig. 9.   Trajectory examples for the predictive horizon at t=11.1s.

Fig. 10.   Trajectory examples for the predictive horizon at t=30.9s.

under ACC will only slow down starting from 3 second to follow OV1 as lane change is not available under this setting. This also shows the potential undesired local minimum for maneuver planning. The predictive speed assignment in the OSM case considers reference speed change on lane 1 as well as the potential reference speed change on lane 2. This can be also seen in Figure 9 which shows the computed trajectories for the prediction horizon at t=11.1s, including the planned relative position, the reference speed assignment, and the lane selection variables. We can see when ACV approaches OV2 (at $11+2 = 13s$), the reference speeds of the OSM case in the prediction horizon (set via the rule-based reference speed automaton of Section IV-B) for lane 2 vary from the desired cruise speed to those of speed of the OV2. This is done as soon as the gaps between the ACV and these OVs are predicted to be smaller than the threshold defined in equation (10). For the same horizon, the OOM case switched only the reference speed for lane 1. The changes of the speed references in the prediction horizon are captured via the switching of $v_{t,r,1}$, $v_{t,r,2}$ and $v_{t,r,2}$ at the left column. These changes gradually increase the value of the objective function and force the ACV to either slow down to follow OV2 or change lane. The weighting parameters listed in Table III promote a lane change maneuver if an open lane is available. The ACV is predictively controlled to steer to lane 3 in this case. The pre-planning of the reference speed changes helps to consider changes in the environment from the beginning and helps the MPC to generate more smooth trajectories.
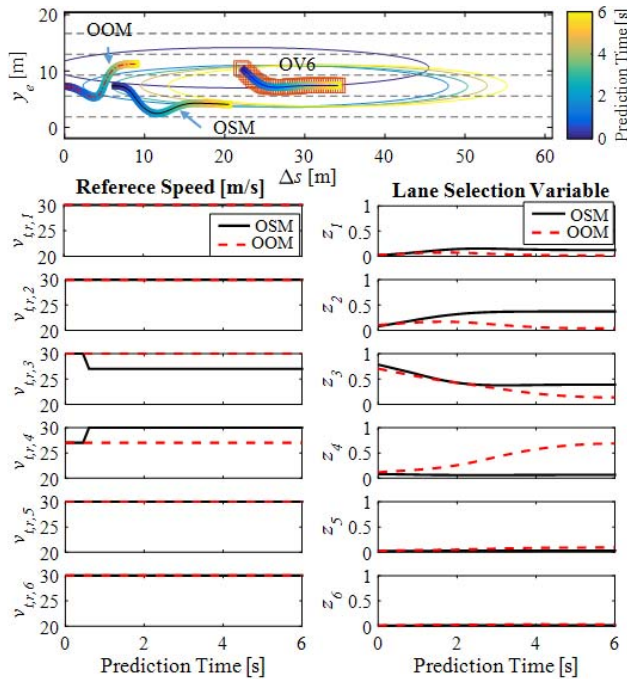
Note that during the lane change, the rise of z_2 is observed in Figure 8, this is due to the fact that ACV needs to go across lane 2 to reach lane 3 and the rise of z_2 actually reduces the value of the objective function. However, z_2 will not rise to 1 because settling down in lane 2 is not the local minimum
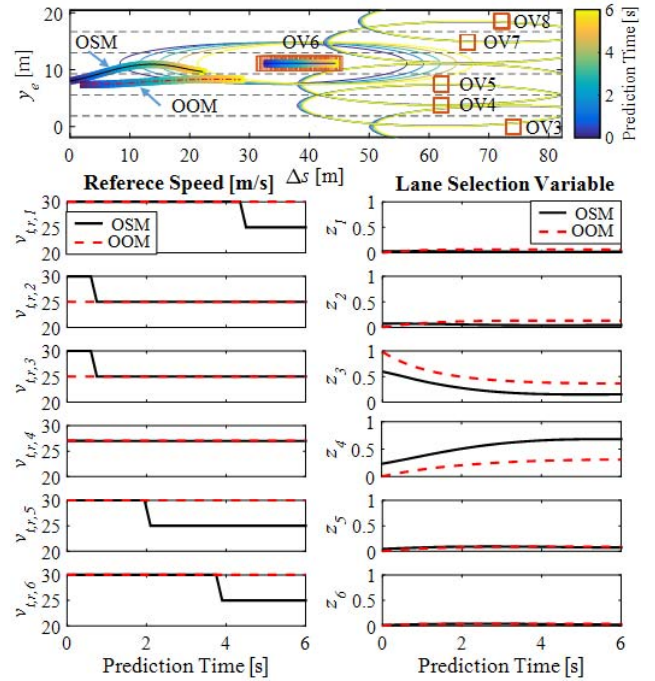
for that moment. The MPC update continues to predictively change lane to lane 3 further reducing the objective function to zero.

2) Overtaking While Following: For the next 40s (20~60s), the ACV faces a "traffic jam" consisting of OV3 in lane 1, OV4 in lane 2, OV5 in lane 3, OV6 in lane 4, OV7 in lane 5 and OV8 in lane 6. Only lane 4 is eventually available to go through. However, the ACV has to change lane to follow a slower OV6 first, because it occupies lane 4 in front of the ACV. As OV6 is faster than the other OVs, it can pass through the "block" together with the ACV. Afterward, the ACV will switch from a following mode (discrete state) to lane change mode in order to overtake the OV6. The details of this operation are as shown in Figure 7, Figure 8 and Figure 10.

From Figure 10, we can see the detailed workings of the ACV detects the "traffic jam" around time=30.9s. Similar as the previous scenario, the ACV with OSM can predict the reference speed switch. The reference speed of the lanes from lane 1 to lane 6, except for lane 4 (which tracks a higher speed 27m/s of OV6), in the predictive horizon switch from 30m/s to 25m/s at different times when the ACV approaches the jam. While in the OOM case only the thresholds of lane 2, 3 and 4 are triggered based on the relative position at that moment. The different speed assignments in the two cases affect their position planning, as shown in the top of Figure 10. For case of OSM, the ACV plan to change lane to lane 4 and follow OV6 with least speed gap to minimize the objective function (zero value local minimum can be achieved). However, in the OOM case, the ACV only has a sideward movement to OV6 to reduce the object function but not strictly following one lane (see the z_3 and z_4 in Figure 10). This lead to the dilemma of the ACV at the joint area of the elliptical boundaries of

This article has been accepted for inclusion in a future issue of this journal. Content is final as presented, with the exception of pagination.

WANG *et al.*: PREDICTIVE MANEUVER PLANNING FOR AN AUTONOMOUS VEHICLE IN PUBLIC HIGHWAY TRAFFIC 11

Fig. 11. Trajectory examples for the predictive horizon at t=78.45s.

Fig. 12. History of MPC execution time.

OV6 and OV5 (non-zero local minimum), which further causes the oscillation of lateral acceleration, lane selection, more speed reduction and slow settling of the objective function between 40s and 50s in Figure 10. Here we can see the predictive maneuver sequence can help achieve a feasible and smoother motion plan which manifests as reduced occupant discomfort and mechanical wear. Finally, when OV6 passes OV5, the ACV gradually goes back to lane 4. Note that as the elliptical collision boundary with 99% uncertainty belief region is not violated during the planning, a collision-free trajectory is achieved.

Afterward, in both cases, the ACV follows the front OV6 until it passes the block/jam. When ACV exceed the other OV(3,4,5,7,8), reference speeds of the related lanes are then reduced by the coefficient of k_l to ensure that tracking these lanes leads to more cost. Therefore, the MPC will command another lane change to lane 3 to overtake OV6 and increase the ACVs speed to 30m/s. Finally, the reference speed of each lane will switch back to the desired cruise speed when ACV passes all the OVs.

3) Collision Avoidance: In the last 15 s, OV6 makes an unexpected sudden lane change starting at time=78 s to the lane occupied by the ACV when the ACV is just overtaking the OV6 from behind. To avoid collision with OV6, the ACV needs to plan its trajectories without entering the elliptical boundary, which might require either slowing down (or speeding up in other situations) in the longitudinal direction and lane change in the lateral direction. The spike in the objective function is mainly due to the sudden braking by the ACV.

From Figure 8, the ACV under OSM and OOM combines both decelerating and lane change to the right to avoid the collision. The future trajectory of the OV6 is predicted at each sampling time, an example for the prediction horizon at
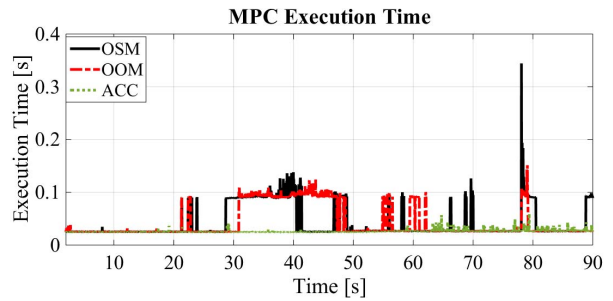
time=78.45 is shown in Figure 11. Based on this, in OSM case, the lane reference speeds from lane 4 to lane 1 are assigned with OV6's speed at the time OV6 is predicted to go across them. The ACV in this case plans to change lane to lane 2 to avoid a collision with lowest cost. While the OOM case can only assign the reference speed based on the estimation of the current lane occupation for OV6, the speed assignment can't match the position prediction of the OV6, therefore its planning decision is more naïve than OSM case. In this case, slowing down and changing lane to lane 4 to track the speed of OV6 is with the lowest cost. When OV6 goes across the boundary between lane 3 and lane 4, change lane to lane 2 became the best planning decision, which matches the results in Figure 7. In both cases, the collision probability during the collision avoidance is close to 0% due to the constraint (25) considering the uncertainties.

Here, we have to point out that the relative positions between OV6 and the ACV when OV6 starts to change lane will affect the maneuver planning results. A closer distance requires faster lane change. That's why the lane change of the ACV in OSM case is more aggressive than the ACV in OOM case. With predictive speed assignment, the ACV can be better prepared for the change of the environment and then make more appropriate planning decisions. If OV6 and ACV are too close to each other, there might be no feasible solution in the MPC that avoids entering the collision boundary.

4) Execution Time: Finally, we comment on the execution times involved in the above simulations. The MPC solver in the ACADO Toolkit is executed on an Intel Dual Core i5-4200M 2.4 GHz processor and 4GB RAM. The execution times for the MPC problem for this simulation are shown in VII. Note that for all the cases compared, the MPC execution times are mostly in the order of 90ms or less; increasing when the elliptical inequality constraints are engaged, more sharply in the initial part of collision avoidance.

VII. SUMMARY AND CONCLUSIONS

This paper outlined, a predictive maneuver planning and control framework that integrates both discrete maneuver planning and motion trajectory planning for an autonomous controlled vehicle in the presence of uncertainties (disturbances and sensor noise). Within the prediction horizon, a rule-based assignment of reference speeds for each reference lane is applied in each interval of the horizon based on the predicted motion of the autonomous vehicle and other object vehicles.

Then, the sequence of maneuvers is incorporated in a relaxed stochastic MPC formulated to simultaneously generate the optimized reference selections and control input trajectories that minimize an objective function subjected to traffic constraints and rules involving other objects that are prevalent in public traffic. A series of simulation experiments showed that, the maneuver planning helps the autonomous vehicle to better accommodate the environment. Also, the modification in the reference speed assignment improves the optimality and the robustness of the maneuver decision in trajectory planning without adding computational complexity to the optimization problem.

Future work will look at: 1) how to approach a formal design of the switching set (automaton) to improve, or if possible guarantee, the feasibility of the MPC in most situations, 2) consider externally controlled switching, such as with interventions from a human driver in a semi-autonomous driving mode or from traffic control devices in a collaborative driving mode. In addition, the broader impact of the proposed predictive maneuver planning on overall traffic efficiency should be evaluated considering heterogeneity of vehicles and other classes of uncertainty than those considered in this paper.

REFERENCES

[1] D. Delling, P. Sanders, D. Schultes, and D. Wagner, "Engineering route planning algorithms," in *Algorithmics of Large and Complex Networks*, vol. 5515. Berlin, Germany: Springer, 2009, pp. 117–139.

[2] D. González, J. Pérez, V. Milanés, and F. Nashashibi, "A review of motion planning techniques for automated vehicles," *IEEE Trans. Intell. Transp. Syst.*, vol. 17, no. 4, pp. 1135–1145, Apr. 2016.

[3] B. Paden, M. Čáp, S. Z. Yong, D. Yershov, and E. Frazzoli, "A survey of motion planning and control techniques for self-driving urban vehicles," *IEEE Trans. Intell. Veh.*, vol. 1, no. 1, pp. 33–55, Mar. 2016. [Online]. Available: https://arxiv.org/pdf/1604.07446.pdf

[4] S. M. LaValle, *Planning Algorithms*. Cambridge, U.K.: Cambridge Univ. Press, 2006.

[5] E. Frazzoli, M. A. Dahleh, and E. Feron, "Maneuver-based motion planning for nonlinear systems with symmetries," *IEEE Trans. Robot.*, vol. 21, no. 6, pp. 1077–1091, Dec. 2005.

[6] A. Kushleyev and M. Likhachev, "Time-bounded lattice for efficient planning in dynamic environments," in *Proc. IEEE Int. Conf. Robot. Automat. (ICRA)*, May 2009, pp. 1662–1668.

[7] Y. Kuwata, J. Teo, G. Fiore, S. Karaman, E. Frazzoli, and J. P. How, "Real-time motion planning with applications to autonomous urban driving," *IEEE Trans. Control Syst. Technol.*, vol. 17, no. 5, pp. 1105–1118, Sep. 2009.

[8] J. Bohren *et al.*, "Little ben: The ben franklin racing team's entry in the 2007 DARPA urban challenge," *J. Field Robot.*, vol. 25, no. 9, pp. 598–614, 2008.

[9] D. Ferguson, T. M. Howard, and M. Likhachev, "Motion planning in urban environments," *J. Field Robot.*, vol. 25, nos. 11–12, pp. 939–960, Nov. 2008.

[10] T. Fraichard and A. Scheuer, "From Reeds and Shepp's to continuous-curvature paths," *IEEE Trans. Robot.*, vol. 20, no. 6, pp. 1025–1035, Dec. 2004.

[11] M. McNaughton, C. Urmson, J. M. Dolan, and J.-W. Lee, "Motion planning for autonomous driving with a conformal spatiotemporal lattice," in *Proc. IEEE Int. Conf. Robot. Automat. (ICRA)*, May 2011, pp. 4889–4895.

[12] L. Han, H. Yashiro, H. T. N. Nejad, Q. H. Do, and S. Mita, "Bézier curve based path planning for autonomous vehicle in urban environment," in *Proc. IEEE Intell. Vehicles Symp.*, Jun. 2010, pp. 1036–1042.

[13] M. Vukov, A. Domahidi, H. J. Ferreau, M. Morari, and M. Diehl, "Auto-generated algorithms for nonlinear model predictive control on long and on short horizons," in *Proc. IEEE 52nd Annu. Conf. Decis. Control*, Florence, Italy, Dec. 2013, pp. 5113–5118.

[14] B. Houska, H. J. Ferreau, and M. Diehl, "An auto-generated real-time iteration algorithm for nonlinear MPC in the microsecond range," *Automatica*, vol. 47, no. 10, pp. 2279–2285, 2011.

[15] G. Prokop, "Modeling human vehicle driving by model predictive online optimization," *Veh. Syst. Dyn.*, vol. 35, no. 1, pp. 19–53, 2001.

[16] P. Falcone, F. Borrelli, J. Asgari, H. E. Tseng, and D. Hrovat, "Predictive active steering control for autonomous vehicle systems," *IEEE Trans. Control Syst. Technol.*, vol. 15, no. 3, pp. 566–580, May 2007.

[17] J. Ziegler, P. Bender, T. Dang, and C. Stiller, "Trajectory planning for Bertha—A local, continuous method," in *Proc. IEEE Intell. Vehicles Symp.*, Jun. 2014, pp. 450–457.

[18] S. J. Anderson, S. C. Peters, T. E. Pilutti, and K. Iagnemma, "An optimal-control-based framework for trajectory planning, threat assessment, and semi-autonomous control of passenger vehicles in hazard avoidance scenarios," *Int. J. Vehicle Auto. Syst.*, vol. 8, nos. 2–4, pp. 190–216, 2010.

[19] T. Weiskircher, Q. Wang, and B. Ayalew, "Predictive guidance and control framework for (semi-)autonomous vehicles in public traffic," *IEEE Trans. Control Syst. Technol.*, vol. 25, no. 6, pp. 2034–2046, Nov. 2017.

[20] A. B. Hillel, R. Lerner, D. Levi, and G. Raz, "Recent progress in road and lane detection: A survey," *Mach. Vis. Appl.*, vol. 25, no. 3, pp. 727–745, 2014.

[21] T. Kowsari, S. S. Beauchemin, and M. A. Bauer, "Map-based lane and obstacle-free area detection," in *Proc. IEEE Int. Conf. Comput. Vis. Theory Appl. (VISAPP)*, Jan. 2014, pp. 523–530.

[22] A. Gray, Y. Gao, T. Lin, J. K. Hedrick, H. E. Tseng, and F. Borrelli, "Predictive control for agile semi-autonomous ground vehicles using motion primitives," in *Proc. Amer. Control Conf.*, Montreal, QC, Canada, 2012, pp. 4239–4244.

[23] D. Q. Mayne, J. B. Rawlings, C. V. Rao, and P. O. M. Scokaert, "Constrained model predictive control: Stability and optimality," *Automatica*, vol. 36, no. 6, pp. 789–814, 2000.

[24] H. Chen and F. Allgöwer, "A quasi-infinite horizon nonlinear model predictive control scheme with guaranteed stability," in *Proc. IEEE Eur. Control Conf. (ECC)*, Jul. 1997, pp. 1421–1426.

[25] S. Lefèvre, D. Vasquez, and C. Laugier, "A survey on motion prediction and risk assessment for intelligent vehicles," *Robomech. J.*, vol. 1, no. 1, 2014.

[26] R. Schubert, E. Richter, and G. Wanielik, "Comparison and evaluation of advanced motion models for vehicle tracking," in *Proc. IEEE Int. Conf. Inf. Fusion*, Jun./Jul. 2008, pp. 1–6.

[27] M. Brännström, E. Coelingh, and J. Sjöberg, "Model-based threat assessment for avoiding arbitrary vehicle collisions," *IEEE Trans. Intell. Transp. Syst.*, vol. 11, no. 3, pp. 658–669, Sep. 2010.

[28] S. Atev, G. Miller, and N. P. Papanikolopoulos, "Clustering of vehicle trajectories," *IEEE Trans. Intell. Transp. Syst.*, vol. 11, no. 3, pp. 647–657, Sep. 2010.

[29] Q. Tran and J. Firl, "Online maneuver recognition and multimodal trajectory prediction for intersection assistance using non-parametric regression," in *Proc. IEEE Intell. Vehicles Symp.*, Jun. 2014, pp. 918–923.

[30] A. Lawitzky, D. Althoff, C. F. Passenberg, G. Tanzmeister, D. Wollherr, and M. Buss, "Interactive scene prediction for automotive applications," in *Proc. IEEE Intell. Vehicles Symp.*, Jun. 2013, pp. 1028–1033.

[31] G. Agamennoni, J. I. Nieto, and E. M. Nebot, "A Bayesian approach for driving behavior inference," in *Proc. IEEE Intell. Vehicles Symp.*, Jun. 2011, pp. 595–600.

[32] N. Dadkhah and B. Mettler, "Survey of motion planning literature in the presence of uncertainty: Considerations for UAV guidance," *J. Intell. Robot. Syst.*, vol. 65, no. 1, pp. 233–246, 2012.

[33] C. Schmidt, F. Oechsle, and W. Branz, "Research on trajectory planning in emergency situations with multiple objects," in *Proc. IEEE Intell. Transp. Syst. Conf.*, Sep. 2006, pp. 988–992.

[34] Y. Kuwata, T. Schouwenaars, A. Richards, and J. How, "Robust constrained receding horizon control for trajectory planning," in *Proc. AIAA Guid., Navigat., Control Conf. Exhibit*, 2005.

[35] P. Falcone, M. Ali, and J. Sjoberg, "Predictive threat assessment via reachability analysis and set invariance theory," *IEEE Trans. Intell. Transp. Syst.*, vol. 12, no. 4, pp. 1352–1361, Dec. 2011.

[36] C. J. Ostafew, A. P. Schoellig, and T. D. Barfoot, "Robust constrained learning-based NMPC enabling reliable mobile robot path tracking," *Int. J. Robot. Res.*, vol. 35, no. 13, pp. 1547–1563, 2016.

[37] M. Althoff, O. Stursberg, and M. Buss, "Model-based probabilistic collision detection in autonomous driving," *IEEE Trans. Intell. Transp. Syst.*, vol. 10, no. 2, pp. 299–310, Jun. 2009.

[38] M. Althoff and J. M. Dolan, "Online verification of automated road vehicles using reachability analysis," *IEEE Trans. Robot.*, vol. 30, no. 4, pp. 903–918, Aug. 2014.

[39] N. E. Du Toit and J. W. Burdick, "Robot motion planning in dynamic, uncertain environments," *IEEE Trans. Robot.*, vol. 28, no. 1, pp. 101–115, Feb. 2012.

[40] M. Farrokhsiar and H. Najjaran, "Unscented model predictive control of chance constrained nonlinear systems," *Adv. Robot.*, vol. 28, no. 4, pp. 257–267, 2014.

[41] E. Mazor, A. Averbuch, Y. Bar-Shalom, and J. Dayan, "Interacting multiple model methods in target tracking: A survey," *IEEE Trans. Aerosp. Electron. Syst.*, vol. 34, no. 1, pp. 103–123, Jan. 1998.

[42] Q. Wang, T. Weiskircher, and B. Ayalew, "Hierarchical hybrid predictive control of an autonomous road vehicle," in *Proc. ASME Dyn. Syst. Control Conf.*, Columbus, HI, USA, 2015, p. V003T50A006.

[43] Q. Wang, B. Ayalew, and T. Weiskircher, "Optimal assigner decisions in a hybrid predictive control of an autonomous vehicle in public traffic," in *Proc. Amer. Control Conf.*, Boston, MA, USA, 2016, pp. 3468–3473.

[44] M. Tsogas, A. Polychronopoulos, N. Floudas, and A. Amditis, "Situation refinement for vehicle maneuver identification and driver's intention prediction," in *Proc. IEEE Int. Conf. Inf. Fusion*, Jul. 2007, pp. 1–8.

[45] V. Gadepally, A. Krishnamurthy, and U. Ozguner, "A framework for estimating driver decisions near intersections," *IEEE Trans. Intell. Transp. Syst.*, vol. 15, no. 2, pp. 637–646, Apr. 2014.

[46] A. Kurt and Ü. Özgüner, "Hierarchical finite state machines for autonomous mobile systems," *Control Eng. Pract.*, vol. 21, no. 2, pp. 184–194, 2013.

[47] T. Weiskircher and B. Ayalew, "Frameworks for interfacing trajectory tracking with predictive trajectory guidance for autonomous road vehicles," in *Proc. Amer. Control Conf.*, Chicago, IL, USA, 2015, pp. 477–482.

[48] A. Micaelli and C. Samson, "Trajectory tracking for unicycle-type and two-steering-wheels mobile robots," INRIA, Paris, France, Res. Rep. RR-2097, 1993.

[49] D. A. Johnson and M. M. Trivedi, "Driving style recognition using a smartphone as a sensor platform," in *Proc. Int. IEEE Conf. Intell. Transp. Syst. (ITSC)*, Oct. 2011, pp. 1609–1615.

[50] S. J. Julier and J. K. Uhlmann, "New extension of the Kalman filter to nonlinear systems," *Proc. SPIE*, vol. 3068, Jul. 1997.

[51] A. Carvalho, Y. Gao, S. Lefèvre, and F. Borrelli, "Stochastic predictive control of autonomous vehicles in uncertain environments," in *Proc. Int. Symp. Adv. Vehicle Control*, 2014, pp. 1–8.

[52] T. Streubel and K. H. Hoffmann, "Prediction of driver intended path at intersections," in *Proc. IEEE Intell. Vehicles Symp.*, Jun. 2014, pp. 134–139.

[53] P. Belotti, C. Kirches, S. Leyffer, J. Linderoth, J. Luedtke, and A. Mahajan, "Mixed-integer nonlinear optimization," *Acta Numer.*, vol. 22, pp. 1–131, 2013.

[54] B. Houska, H. J. Ferreau, and M. Diehl, "ACADO toolkit—An open-source framework for automatic control and dynamic optimization," *Optim. Control Appl. Methods*, vol. 32, no. 3, pp. 298–312, 2011.

[55] H. J. Ferreau, "Model predictive control algorithms for applications with millisecond timescales," Ph.D. dissertation, Dept. Elect. Eng., KU Leuven, Leuven, Belgium, 2011.

[56] T. Weiskircher and B. Ayalew, "Predictive trajectory guidance for (semi-)autonomous vehicles in public traffic," in *Proc. Amer. Control Conf.*, Chicago, IL, USA, 2015, pp. 3328–3333.

[57] J. Ziegler and C. Stiller, "Spatiotemporal state lattices for fast trajectory planning in dynamic on-road driving scenarios," in *Proc. IEEE/RSJ Int. Conf. Intell. Robots Syst. (IROS)*, Oct. 2009, pp. 1879–1884.

Qian Wang received the Diploma and master's degrees in vehicle engineering from South China University of Technology, Guangzhou, China, in 2013 and the Ph.D. degree in automotive engineering from Clemson University in 2017. Since 2017, he has been an Autonomous Driving Research and Development Engineering with Aptiv (formerly known as delphi). His research interests include optimal control, predictive trajectory planning and control for autonomous vehicles, and control allocation for vehicle actuation systems.

Beshah Ayalew received the M.S. and Ph.D. degrees in mechanical engineering from Pennsylvania State University in 2000 and 2005, respectively. He is currently a Professor of automotive engineering and the Director of the DOE GATE Center of Excellence in Sustainable Vehicle Systems, Clemson University. His interest and expertise is in systems dynamics and controls. He is an active member of the ASME's Vehicle Design Committee, the IEEE's Control Systems Society, and SAE. He received the Ralph Teetor Educational Award from SAE (2014), the Clemson University Board of Trustees Award for Faculty Excellence (2012), and the NSF CAREER Award (2011). He was a recipient of the Penn State Alumni Association Dissertation Award (2005).

Thomas Weiskircher received the Diploma degree in mechatronics engineering from Universität des Saarlandes, Saarbrücken, Germany, in 2009 and the Ph.D. degree in mechanical engineering from Technische Universität Kaiserslautern, Kaiserslautern, Germany, in 2013. He was a Post-Doctoral Research in vehicle control with the Applied Dynamics and Control Research Group, Clemson University International Center of Automotive Research, Greenville, SC, USA, from 2014 to 2015. Since 2015, he has been a Research and Advanced Engineer at Dimlar AG, Böblingen, Germany. His current research interests include optimal control, real-time model predictive control for automotive applications, vehicle dynamics control, and active safety systems.